A Drift-Diffusion-Based Analytic Description of the Energy Distribution Function for Hot-Carrier Degradation in Decananometer nMOSFETs

Prateek Sharma, Stanislav Tyaginov, Stewart E. Rauch III, *Senior Member, IEEE*, Jacopo Franco, *Member, IEEE*, Ben Kaczer, Alexander Makarov, Mikhail I. Vexler, Tibor Grasser, *Fellow, IEEE*

***Abstract*—We extend our drift-diffusion based model for the carrier energy distribution function (DF), which was derived to describe hot-carrier degradation in LDMOS transistors, for the case of decananometer nMOSFETs with a gate length of 65 nm. This approach is based on an analytical expression for the DF with parameters obtained from the drift-diffusion model. To approximately consider the important effect of electron-electron scattering on the shape of the distribution function, we solve the balance equation for the in- and out-scattering rates. We compare the DFs obtained from the suggested analytic approach with those calculated with a deterministic Boltzmann transport equation solver. Both sets of DFs are then used in our hot-carrier degradation model to calculate changes in the linear drain current as a function of stress time. Good agreement with experimental data is achieved for both versions of the model.**

***Index Terms*—hot-carrier degradation, nMOSFET, electron-electron scattering, drift-diffusion scheme, analytic energy distribution function**

I. Introduction

During the last two decades the paradigm of hot-carrier degradation (HCD) has changed from field driven approaches such as the lucky electron model [1] to the energy driven concept proposed by Rauch and LaRosa [2, 3]. In particular, our recent HCD modeling results suggest that the entire Si-H bond-breakage process, which is assumed to be the dominant contributor to device degradation, is described by the carrier energy distribution function (DF) [4, 5]. The carrier distribution function can be obtained from a solution of the Boltzmann transport equation (BTE), which is computationally very expensive [6]. There are two frequently used approaches for the solution of the BTE: the stochastic approach based on the Monte-Carlo method and a deterministic approach which uses the spherical harmonics expansion of the DF. The latter technique has a number of advantages: it allows to better resolve the high-energy tails of the DF (which are of crucial importance in the context of HCD), simulate long-channel devices under high operating/stress voltages in a reasonable time, and implement electron-electron scattering (EES) in a more straightforward manner. It has been previously shown that EES plays a crucial role in hot-carrier degradation of short-channel devices [7–10]. This process populates the high-energy fraction of the carrier ensemble, thereby considerably changing the shape of the carrier DF, which is visible in a characteristic hump pronounced at high energies [3, 11]. Apparently EES also determines the temperature behavior of HCD in scaled devices [3, 12].

The solution of the BTE is a challenging task, and many HCD modeling approaches try to avoid it by using simplified techniques of carrier transport treatment such as the drift-diffusion and energy transport schemes [13, 14]. Recently we have developed an HCD model based on the drift-diffusion scheme which can accurately describe HCD in high-voltages devices, namely in LDMOS transistors [14, 15]. We also have studied the limits of the applicability of the model and shown that in the case of planar nMOSFETs the model fails to capture HCD in transistors with a gate length of shorter than 1.5 μm [16] which is consistent with our previous results [17].

Here we extend our drift-diffusion model for the carrier energy distribution function [14, 15] to make it suitable for decananometer nMOSFETs with a gate length of 65 nm. Special attention is paid to the impact of EES on the DF shape. The electron DFs simulated with this model will be compared to those obtained from our deterministic solver ViennaSHE [18]. We also compare the degradation of the linear drain current computed with the two different versions of the DF and experimental data.

II. The Distribution Function Model

Our HCD model [10, 12] describes the kinetics of interface state generation by hot-carriers. The bond-breakage rate is determined by the carrier DF which is the primary ingredient of our model. Three sets of carrier DFs evaluated with ViennaSHE for three different stress conditions (V_{gs} = V_{ds} = 1.8, 2.0, 2.2 V) are shown in Fig. 1. One can see that the DF shape substantially changes if one moves from the source to the drain, see Fig. 2. Indeed, DFs evaluated near the source and in the channel have a maximum visible at low and moderate energies with the corresponding energy labeled as $\varepsilon_{\mathrm{k},1}$. As for the drain DFs, they typically feature a Maxwellian rudiment visible at low energies followed by a plateau. The end of this plateau also corresponds to the knee energy $\varepsilon_{\mathrm{k},1}$, see Fig. 2. Another characteristic energy where the DF changes

P. Sharma, A. Makarov, and T. Grasser are with the Institute for Microelectronics, Technische Universität Wien, 1090 Vienna, Austria.

S. Tyaginov is with the Institute for Microelectronics, Technische Universität Wien, 1090 Vienna, Austria and also with the Ioffe Physical-Technical Institute, Russian Academy of Sciences, St. Petersburg 194021, Russia.

S. Rauch is with GlobalFoundries, New York 12533, USA.

J. Franco and B. Kaczer are with imec, Leuven 3001, Belgium.

M. Vexler is with the Ioffe Physical-Technical Institute, Russian Academy of Sciences, St. Petersburg 194021, Russia.

978-1-5090-2969-3/16/$31.00 ©2016 IEEE

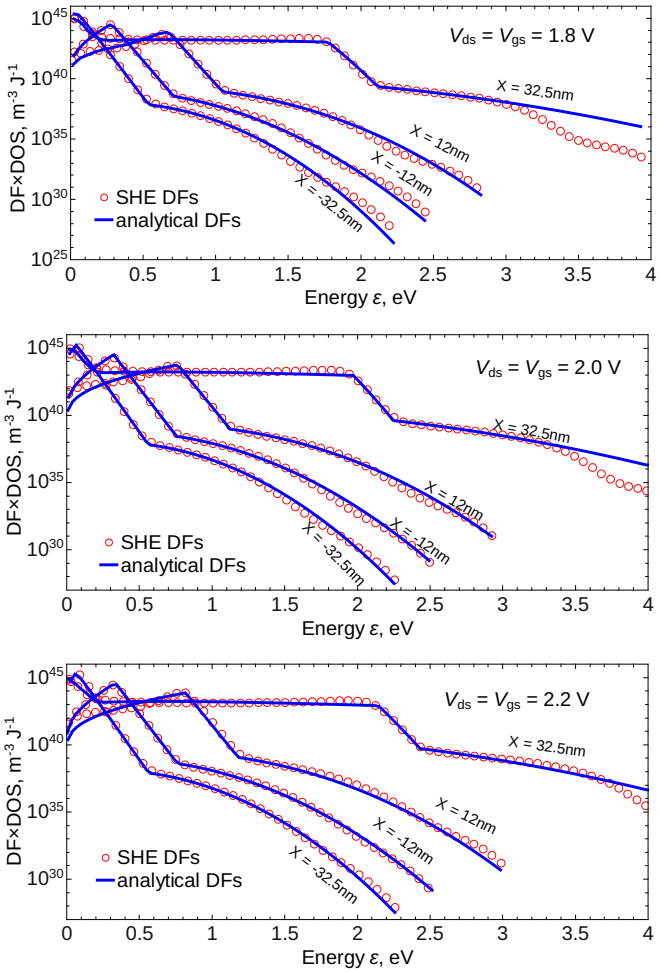

Fig. 1: Comparison of carrier distribution functions calculated with ViennaSHE and our DD-based method for three different stress conditions V_{gs} = V_{ds} = 1.8 V, 2.0 V, and 2.2 V. DFs are plotted for four different positions in the device (x = -32.5 nm corresponds to the source, while x = 32.5 nm is related to the drain).

its curvature is related to the onset of the EES hump and is labeled as $\varepsilon_{k,2}$.

The distribution function is modeled using our DD-based approach and is determined by [14]:

$$f(\varepsilon) = A\exp\left[-\left(\frac{\varepsilon}{\varepsilon_{\mathrm{ref}}}\right)^{b}\right] + C\exp\left[-\frac{\varepsilon}{k_{\mathrm{B}}T_n}\right]. \qquad (1)$$

This DF expression accounts for both the hot and cold carriers in the device. The parameters A, $\varepsilon_{\mathrm{ref}}$, C in (1) are obtained from the moments of the BTE calculated using DD simulations such as the carrier concentration and carrier temperature and DF normalization, while for parameter b a different value is used after every knee position, see Fig. 2. In the channel and source region b assumes a value of -1 before $\varepsilon_{k,1}$, 1 between $\varepsilon_{k,1}$ and $\varepsilon_{k,2}$, and 2 after $\varepsilon_{k,2}$. While for the drain region, b has a value of 0.2 before $\varepsilon_{k,1}$, 1 between $\varepsilon_{k,1}$ and $\varepsilon_{k,2}$, and 2 after $\varepsilon_{k,2}$. The carrier temperature is estimated from the homogeneous energy balance using the electric field [19].

Eq. (1) allows for a rough evaluation of the electron DF without the effect of electron-electron scattering. This DF is then used to calculate the knee energy $\varepsilon_{k,2}$ and describe the

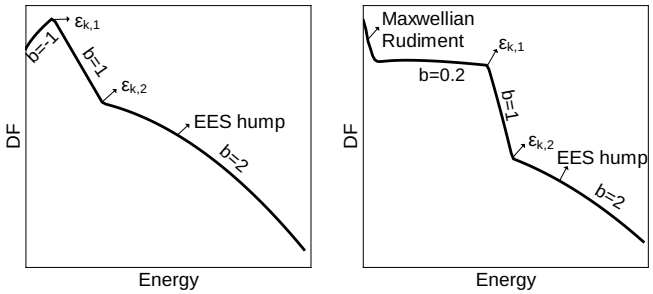

Fig. 2: A schematic representation of the carrier DFs for the channel area (left panel) and for the drain (right panel) with all characteristic peculiarities marked.

impact of EES on the DF shape as discussed below.

The first knee energy in the low energy region is evaluated analytically using the electric field from the DD simulations:

$$\varepsilon_{k,1} = \alpha\exp[\beta - \gamma F]^{\frac{1}{2}}, \qquad (2)$$

where F is the electric field, while α, β, and γ are fitting parameters with values 0.1982 eV, 8.251, 1.51×10^{-6} cmV^{-1}, respectively.

The second knee energy, where EES starts to dominate the high energy tail, is obtained by considering the balance of in-scattering by EES and out-scattering by electron-phonon interactions and ionized impurity scattering [20, 21]:

$$r_{\mathrm{ees}} = r_{\mathrm{ii}} + r_{\mathrm{op/abs}} + r_{\mathrm{op/emi}} + r_{\mathrm{acc}} \qquad (3)$$

The acoustic phonon scattering rate is given as [22]:

$$r_{\mathrm{acc}} = \frac{D_{\mathrm{A}}^2 k_{\mathrm{B}} T_{\mathrm{L}} m^* p}{\pi c_{\mathrm{l}} \hbar^4}, \qquad (4)$$

where D_{A} is the acoustic deformation potential, c_{l} the elastic constant ($v_{\mathrm{s}} = \sqrt{c_{\mathrm{l}}/\rho}$, v_{s} the velocity of sound and ρ stands for the mass density). For spherical parabolic bands $p = \sqrt{2m^*\varepsilon}$. Note that for a fair comparison the same physical parameters are used in both the SHE code and the analytic approximation.

Optical phonon scattering can be due to absorption or emission of the optical phonons. The corresponding rates are

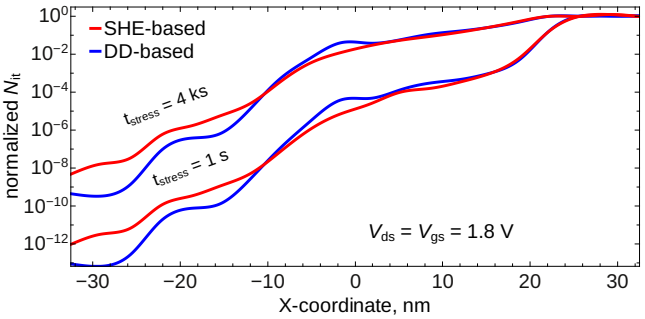

Fig. 3: The interface state density profiles $N_{\mathrm{it}}(x)$, normalized to the concentration of pristine Si-H bond , evaluated using DFs obtained with our analytic model and using ViennaSHE. Stress voltages are V_{gs} = V_{ds} = 1.8 V. The profiles are shown for stress times of 1 s and 4 ks.

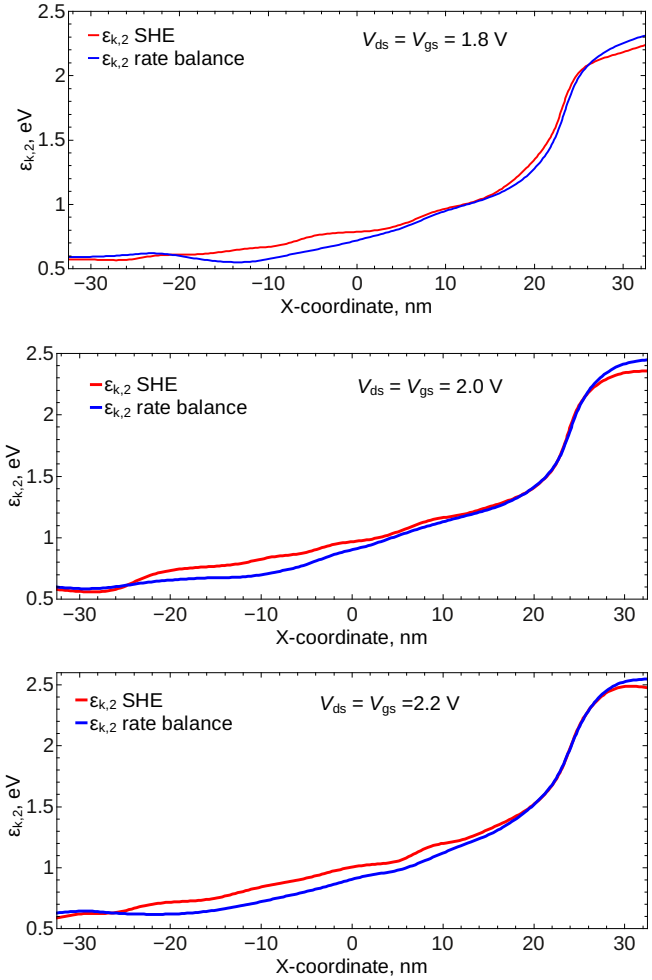

Fig. 4: The knee energy $\varepsilon_{\mathrm{k},2}$, where EES starts to dominate the high-energy tail of the carrier DF, calculated with the analytic model plotted vs. those extracted from ViennaSHE results for three different stress conditions V_{gs} = V_{ds} = 1.8 V, 2.0 V, and 2.2 V.

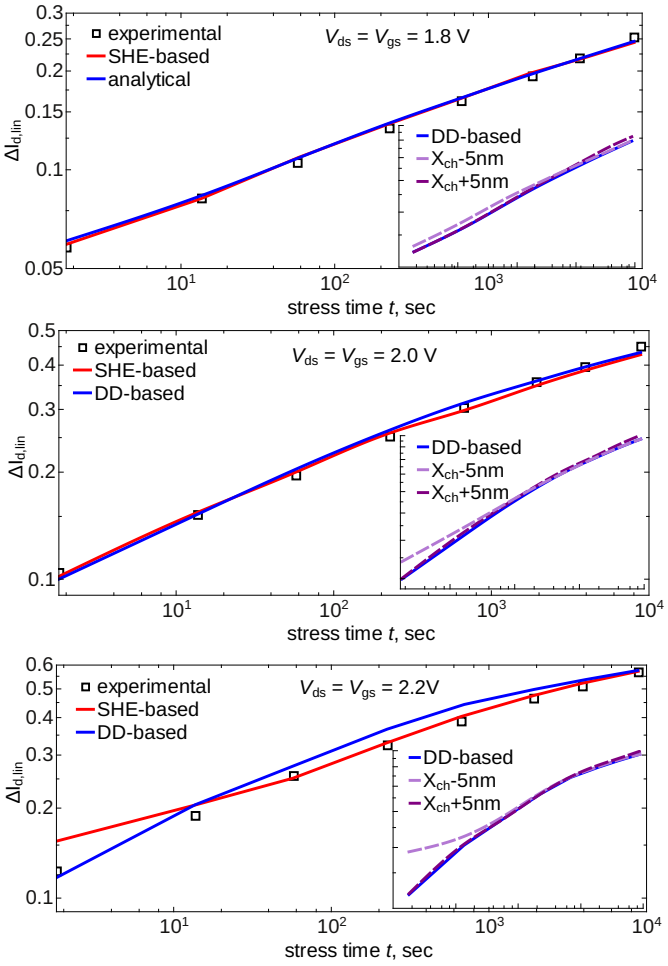

Fig. 5: The normalized change in the linear drain current $\Delta I_{\mathrm{d,lin}}$ as a function of stress time for V_{gs} = V_{ds} = 1.8 V, 2.0 V, and 2.2 V: experiment vs. simulations. Inset: $\Delta I_{\mathrm{d,lin}}$ traces simulated with varied x-coordinate where the DF changes shape (X_{ch}).

given by (5) and (6), respectively [22]:

$$r_{\mathrm{op/abs}} = \frac{D_{\mathrm{o}}^2 N_{\mathrm{o}} m^* \sqrt{2m^* \left(\varepsilon + \hbar\omega_{\mathrm{o}}\right)}}{2\pi\rho\omega_{\mathrm{o}}\hbar^3}, \tag{5}$$

$$r_{\mathrm{op/emi}} = \frac{D_{\mathrm{o}}^2 \left(N_{\mathrm{o}} + 1\right) m^* \sqrt{2m^* \left(\varepsilon - \hbar\omega_{\mathrm{o}}\right)}}{2\pi\rho\omega_{\mathrm{o}}\hbar^3}, \tag{6}$$

where D_{o} is the optical deformation potential, $\hbar\omega_{\mathrm{o}}$ the energy of optical phonons, while N_{o} is the density of optical phonons, $N_{\mathrm{o}} = 1/\left(\exp\left[\hbar\omega_{\mathrm{o}}/k_{\mathrm{B}}T_{\mathrm{L}}\right] - 1\right)$.

The ionized impurity scattering rates are [22]:

$$r_{\mathrm{ii}} = \frac{N_{\mathrm{I}} q^4}{16\sqrt{2m^*}\pi\left(\epsilon_{\mathrm{Si}}\epsilon_0\right)^2}\left[\ln\left(1+\gamma^2\right) - \frac{\gamma^2}{1+\gamma^2}\right]\frac{1}{\varepsilon^{3/2}}, \tag{7}$$

where $\gamma^2 = 8m^*\varepsilon L_{\mathrm{D}}^2/\hbar^2$ with L_{D} being the Debye length given as $L_{\mathrm{D}} = \sqrt{\epsilon_{\mathrm{Si}}\epsilon_0 k_B T/q^2 n_0}$.

As for electron-electron scattering, we use the following expression [23]:

$$r_{\mathrm{EES}} = \frac{mq^4 n}{\epsilon_{\mathrm{Si}}^2\epsilon_0^2\hbar^3}\sum_{\varepsilon}\frac{\sqrt{2m^*}/\hbar\left|\sqrt{\varepsilon} - \sqrt{\varepsilon_0}\right|}{\beta_{\mathrm{D}}^2\left(\frac{2m^*}{\hbar^2}\left(\varepsilon - \varepsilon_0\right) + \beta_{\mathrm{D}}^2\right)} f\left(\varepsilon\right) \tag{8}$$

where β_{D} is the inverse Debye length, i.e. $\beta_{\mathrm{D}} = 1/L_{\mathrm{D}}$. It is important to emphasize that calculation of the rate r_{EES} requires a DF. For this, we employ the distribution (1). EES perturbs the DF, populating the high energy region of the carrier ensemble. This means that for energies $E < \varepsilon_{\mathrm{k},2}$ the DF calculated with (1) can be used, while for $E \geq \varepsilon_{\mathrm{k},2}$ the DF is perturbed due to EES. Once the knee energies are obtained, the DFs are evaluated by changing the value of the parameter b at the knees in Eq. (1). The carrier DFs obtained from ViennaSHE and the analytic method are used with our HCD model [9, 10] to calculate the interface state density ($N_{\mathrm{it}}(x)$) profiles (e.g. Fig. 3). These $N_{\mathrm{it}}(x)$ profiles are then used to simulate the characteristics of the degraded device.

III. Results and Discussion

Fig. 1 shows very good agreement between the DFs simulated with our drift-diffusion based approach and with ViennaSHE for all combinations of V_{gs} and V_{ds}. Incorporation of the knee energies allows for an accurate representation of the high-energy tails and in particular the effect of EES. The values of $\varepsilon_{\mathrm{k},2}$ calculated with the analytic model are almost the same as those obtained from ViennaSHE, see Fig. 4, thereby

suggesting the validity of the rate balance method. After the second knee energy the analytic DFs show a visible error. However, the concentrations at these energies are quite low and do not affect hot-carrier degradation.

To validate the model, we use HCD data acquired on SiON nMOSFETs with a gate length of 65 nm. The devices were stressed under three different stress conditions, i.e. $V_{\rm gs}$ = $V_{\rm ds}$ = 1.8 V, 2.0 V, 2.2 V, at room temperature for ∼8 ks. The relative changes in the linear drain current $\Delta I_{\rm d,lin}(t)$ were recorded as a function of the stress time. The interface state density profiles based on the two different sets of electron DFs for $V_{\rm gs}$ = $V_{\rm ds}$ = 1.8 V, and t = 1 s and 4 ks are plotted in Fig. 3. A slight discrepancy is visible at $x \sim -5$ nm and might be due to the discrepancy in the DFs in the scattering dominated region. This discrepancy, however, does not translate into a model error: Fig. 5 shows that simulated $\Delta I_{\rm d,lin}(t)$ trances are almost identical and are in very good agreement with experimental data. To check the robustness of the model, we vary the value of the coordinate where the DF changes shape ($X_{\rm ch}$) and calculate the $\Delta I_{\rm d,lin}(t)$ traces. A change of 5 nm in $X_{\rm ch}$ impacts the degradation traces (Fig. 5, insets) considerably. This suggests that $X_{\rm ch}$ is an important model parameter for description of the DF shape accurately in all device regions.

IV. Conclusions

We have presented and verified a drift-diffusion based analytical model for the carrier energy distribution function (DF) in decananometer nMOSFETs. Our model properly incorporates the effect of electron-electron scattering (EES) on the DF shape. EES is known to dominate the high-energy tails of the DF which results in a characteristic hump. The energy which corresponds to the onset of this hump is called "knee energy" and is described by the balance equation for in- and out-scattering rates. The distribution functions evaluated by our analytic model and those obtained using the deterministic BTE solver ViennaSHE are almost identical. Furthermore, good agreement between the degradation characteristics obtained with the analytic approach and measurement data suggests that the efficient analytic model is well suited for describing hot-carrier degradation in decananometer devices. Three of our model parameters are found by the solution of the normalization equations, while b is a fitting parameter. This makes the model flexible and efficient. Our new approach allows to avoid time consuming calculations of the carrier distribution function and to model hot-carrier degradation in scaled transistors using the fast drift-diffusion scheme.

Acknowledgments

The authors acknowledge support by the Austrian Science Fund (FWF, grants P23598 and P26382), by the European Union FP7 project ATHENIS_3D (grant No 619246) and by the European Research Council (ERC) project MOSILSPIN (grant No 247056).

References

[1] C. Hu, "Lucky Electron Model for Channel Hot Electron Emission," in *Proc. International Electron Devices Meeting (IEDM)*, 1979, pp. 22–25.

[2] S. Rauch and G. L. Rosa, "The Energy-Driven Paradigm of NMOSFET Hot-Carrier Effects," *IEEE Trans. Dev. Material. Reliab.*, vol. 5, no. 4, pp. 701–705, 2005.

[3] ——, "CMOS Hot Carrier: From Physics to End Of Life Projections, and Qualification," in *Proc. International Reliability Physics Symposium (IRPS), tutorial*, 2010.

[4] S. Tyaginov, I. Starkov, H. Enichlmair, J. Park, C. Jungemann, and T. Grasser, "Physics-Based Hot-Carrier Degradation Models (invited)," *ECS Trans.*, vol. 35, no. 4, pp. 321–352, 2011.

[5] S. Tyaginov and T. Grasser, "Modeling of Hot-Carrier Degradation: Physics and Controversial Issues," in *Proc. International Integrated Reliability Workshop (IIRW)*, 2012, pp. 206–215.

[6] C. Jungemann and B. Meinerzhagen, *Hierarchical Device Simulation*. Springer Verlag Wien/New York, 2003.

[7] S. Rauch, F. Guarin, and G. La Rosa, "Impact of E-E Scattering to the Hot Carrier Degradation of Deep Submicron NMOSFETs," *IEEE Electron Dev. Lett.*, vol. 19, no. 12, pp. 463–465, 1998.

[8] S. Rauch, G. La Rosa, and F. Guarin, "Role of E-E Scattering in the Enhancement of Channel Hot Carrier Degradation of Deep-Submicron NMOSFETs at high $V_{\rm gs}$ Conditions," *IEEE Trans. Dev. Material. Reliab.*, vol. 1, no. 2, pp. 113–119, 2001.

[9] S. Tyaginov, M. Bina, J. Franco, D. Osintsev, O. Triebl, B. Kaczer, and T. Grasser, "Physical Modeling of Hot-Carrier Degradation for Short- and Long-Channel MOSFETs," in *Proc. International Reliability Physics Symposium (IRPS)*, 2014, pp. XT.16–1–16–8.

[10] M. Bina, S. Tyaginov, J. Franco, Y. Wimmer, D. Osinstev, B. Kaczer, T. Grasser *et al.*, "Predictive Hot-Carrier Modeling of n-channel MOSFETs," *IEEE Trans. Electron Dev.*, vol. 61, no. 9, pp. 3103–3110, 2014.

[11] S. Tyaginov, M. Bina, J. Franco, Y. Wimmer, D. Osintsev, B. Kaczer, and T. Grasser, "A Predictive Physical Model for Hot-Carrier Degradation in Ultra-Scaled MOSFETs," in *Proc. Simulation of Semiconductor Processes and Devices (SISPAD)*, 2014, pp. 89–92.

[12] S. Tyaginov, M. Jech, J. Franco, P. Sharma, B. Kaczer, and T. Grasser, "Understanding and Modeling the Temperature Behavior of Hot-Carrier Degradation in SiON nMOSFETs," *IEEE Electron Device Letters*, vol. 37, no. 1, pp. 84–87, 2016.

[13] S. Reggiani, S. Poli, M. Denison, E. Gnani, A. Gnudi, G. Baccarani, S. Pendharkar, and R. Wise, "Physics-Based Analytical Model for HCS Degradation in STI-LDMOS Transistors," *IEEE Trans. Electron Dev.*, vol. 58, pp. 3072–3080, 2011.

[14] P. Sharma, S. Tyaginov, Y. Wimmer, F. Rudolf, K. Rupp, M. Bina, H. Enichlmair, J.-M. Park, R. Minixhofer, H. Ceric, and T. Grasser, "Modeling of Hot-Carrier Degradation in nLDMOS Devices: Different Approaches to the Solution of the Boltzmann Transport Equation," *IEEE Trans. Electron Dev.*, vol. 62, no. 6, pp. 1–8, 2015.

[15] P. Sharma, S. Tyaginov, M. Jech, Y. Wimmer, F. Rudolf, H. Enichlmair, J.-M. Park, H. Ceric, and T. Grasser, "The Role of Cold Carriers and the Multiple-Carrier Process of SiH bond Dissociation for Hot-carrier Degradation in n- and p-channel LDMOS Devices," *Solid-State Electronics*, vol. 115, Part B, pp. 185–191, 2016.

[16] M. Jech, P. Sharma, S. Tyaginov, F. Rudolf, and T. Grasser, "On the Limits of Applicability of Drift-Diffusion Based Hot Carrier Degradation Modeling," *Japanese Journal of Applied Physics*, vol. 55, no. 4S, pp. 04ED14–1–04ED14–6.

[17] S. Tyaginov, I. Starkov, C. Jungemann, H. Enichlmair, J. Park, and T. Grasser, "Impact of the Carrier Distribution Function on Hot-Carrier Degradation Modeling," in *Proc. European Solid-State Device Research Conference (ESSDERC)*, 2011, pp. 151–154.

[18] M. Bina, K. Rupp, S. Tyaginov, O. Triebl, and T. Grasser, "Modeling of Hot Carrier Degradation Using a Spherical Harmonics Expansion of the Bipolar Boltzmann Transport Equation," in *Proc. International Electron Devices Meeting (IEDM)*, 2012, pp. 713–716.

[19] T. Grasser, T.-W. Tang, H. Kosina, and S. Selberherr, "A Review of Hydrodynamic and Energy-Transport Models for Semiconductor Device Simulation," *Proceeding of the IEEE*, vol. 91, no. 2, pp. 251–273, 2003.

[20] D. Ventura, A. Gnudi, and G. Baccarani, "An Efficient Method for Evaluating the Energy Distribution of Electrons in Semiconductors Based on Spherical Harmonics Expansion," *IEICE Trans. Electron.*, vol. E75-C, no. 2, pp. 194–199, 1992.

[21] P. Childs and C. Leung, "New Mechanism of Hot Carrier Generation in Very Short Channel MOSFETs," *Electronics Letters*, vol. 31, no. 2, pp. 139–141, 1995.

[22] M. Lundstrom, *Fundamentals of Carrier Transport*, 2nd ed. Cambridge University Press, 2000.

[23] C. Jacoboni and P. Lugli, *The Monte Carlo Method for Semiconductor Device Simulation*. Springer-Verlag-Wien, 1989.